Supporting Information

High-performance free-standing hydrogen evolution electrodes: riveting tungsten carbide nanocrystals to graphite felt fabrics by carbon nanosheets

Yi Shen*, Ling Li, Jingyu Xi* and Xinping Qiu*

Experimental Section

Synthesis of CNS@WC/GF CNS@WC/GF monoliths were synthesized via in-situ carburization of PTA-loaded GF fabrics in the presence of methane. Prior to synthesis, graphite felt monoliths with a dimension of 1.5 × 1.5 × 0.5 cm were thermally treated using a muffle furnace at 430 ºC for 24 h. 1 g of PTA powder and 20 mL of ethanol were added into a petri dish to form a solution. 10 pieces of activated graphite felts were immersed into the solution. To transfer PTA into graphite felts, the solvent, *i.e.*, ethanol was slowly evaporated at 40 ºC overnight. After the complete evaporation of ethanol, most of the PTA was deposited into graphite felts. The resulting PTA-loaded GF monoliths were transferred into a quartz tube reactor.[1] The system was flushed with nitrogen gas (purity > 99.99%) to remove the air and the reactor was heated to 600 ºC with a ramp rate of 2 ºC min^{-1} under nitrogen flow (flow rate: 50 mL min^{-1}). Then, methane gas (purity > 99.9%) was introduced into the reactor with a flow rate of 50 mL min^{-1}. Meanwhile, the reactor was heated to 900 ºC and hold at this temperature for 4 h. Subsequently, the reactor was cooled to ambient temperature at a rate of 2 ºC min^{-1}.

Structural Characterization A field emission scanning electron microscope (FESEM) (JSM–7600F, JEOL) and transmission electron microscope (TEM) (JEM2010, JEOL) were used to observe the morphologies of the samples. An EDX analyzer equipped in the FESEM and an axis-ultra X-ray photoelectron spectrometer with monochromatized Al-Kα radiation were used to analyze the elemental composition of the samples. X-ray diffraction (XRD) patterns were obtained by a diffractometer (PW1830, Philips) equipped with Cu-Kα radiation of 1.54 Å. Raman spectra were recorded with a Renishaw Raman microscope using 633-nm

excitation at room temperature. To prepare the samples for Raman tests, the CNS@WC was detached from the GF support by intense ultrasonication. The isolated carbon nanosheets were obtained using a sedimentation separation method. The resulting CNS@WC and isolated carbon nanosheets were deposited to silicon wafers and characterized by Raman spectroscopy. For each sample, at least five tests were conducted at different locations. The N_2 adsorption–desorption isotherm was obtained using the accelerated surface area porosimetry system (ASAP 2020, Micromeritics). Thermogravimetric analyses (TGA) were conducted at a temperature range of 50 to 1000°C using a heating rate of 20°C min^{-1} under air flow.

Electrochemical measurements Electrochemical measurements were performed on an electrochemical station equipped with a three-electrode cell as described in our previous work.[2] Prior to test, CNS@WC/GF monoliths were electrochemical activated to enhance the hydrophilicity. A piece of CNS@WC/GF monolith mounted by a home-made clamper was used as working electrode. A saturated calomel electrode (SCE) and graphite plate were used as reference and counter electrodes, respectively. For comparison, a commercial Pt plate (effective geometric area 1 × 1 cm) was also tested. The details of experimental procedures were reported in our previous work. In the experiments, the electrolyte (1M KOH or 1M H_2SO_4) was bubbled with nitrogen gas (purity > 99.99%) and subjected to continuous magnetic stirring. All the potentials reported in this work were referenced to a reversible hydrogen electrode (RHE) by adding a value of (0.241 + 0.059 pH) V. All the electrochemical measurements were conducted at room temperature (298 ± 1 K).

Table S1 Summary of catalytic performance of tungsten carbide-based HER catalysts in acidic solutions

Sample	Catalytic performance	Experimental conditions	Ref.
WC-CNTs	η_o: 15 mV; η_{10}: 145 mV; $j_{300\ mV}$: 117.6 mA cm^{-2}; Tafel slope: 72 mV dec^{-1}	Electrolyte: 0.5 M H_2SO_4; Scan rate: 50 mV s^{-1}	3
Porous WC films	η_o: 120 mV; Tafel slope: 76 mV dec^{-1};	Electrolyte: 0.5 M H_2SO_4; Scan rate: 5 mV s^{-1}	4
GnP-supported tungsten carbide–nitride	η_{10}: 120 mV; Tafel slope: 68.6 mV dec^{-1}	Electrolyte: 0.1 M $HClO_4$; Scan rate 2 mV s^{-1}	5
Bulk W_2C:	η_{10}: 336 mV; Tafel slope: 88.0 mV dec^{-1}		
W_2C/XC	η_{10}: 223 mV		
W_2C/GnP	η_{10}: 186 mV; Tafel slope: 64.7 mV dec^{-1}		
WC microspheres	η_o: 80 mV; Tafel slope: 89 mV dec^{-1}; j_0: 0.179 mA cm^{-2}	Electrolyte: 0.5 M H_2SO_4; Scanning rate: 5 mV s^{-1}	6
WC-CNT	η_{10}: 489 mV; Tafel slope: 122 mV dec^{-1}	Electrolyte: 0.05 M H_2SO_4; Scan rate: 10 mV s^{-1}	7
W-CNT	η_{10}: 435 mV; Tafel slope: 103 mV dec^{-1}		
WC nanowires	j_0: 6.8*10^{-4} mA cm^{-2} Tafel slop: 82 mV dec^{-1}	Electrolyte: 0.5 M H_2SO_4; Scan rate: 5 mV s^{-1}	9
W_4MoC nanowire:	j_0: 2.9*10^{-2} mA cm^{-2} Tafel slop: 52 mV dec^{-1}		
70M2S/30WC-Graphene	η_o: 110 mV; Tafel slope: 41 mV dec^{-1}	Electrolyte: 0.5 M H_2SO_4	10
β-$Mo_{0.06}W_{0.94}C$/CB	$j_{\eta=290\ mV}$: 27 mA; $\eta_{j=1\ mA}$: 156 mV	Electrolyte: H_2-saturated 0.5 M H_2SO_4; Scan rate: 2 mV s^{-1}	11
α-WC/CB	$j_{\eta=290\ mV}$: 21 mA; $\eta_{j=1\ mA}$: 165 mV		
WC	η_o: 184 mV; η_{20}: 444 mV	Electrolyte: 0.1 M H_2SO_4; Scan rate: 5 mV s^{-1}	12
WC	η_o≈244 mV; $j_{344\ mV}$: 0.725 mA cm^{-2}; Tafel slope: 137.1 mV dec^{-1}	Electrolyte: 0.1 M $HClO_4$; Scan rate: 2 mV s^{-1}	13
Carbon coated cobalt–tungsten carbide Co_6W_6C	η: 200 mV; Tafel slope: 75 mV dec^{-1}; j_0: 0.0286 mA cm^{-2}	Electrolyte: 0.5 M H_2SO_4 Scan rate: 50 mV s^{-1}	14
WC-WN decorated graphene	η_{10}: 105 mV; Tafel slope: 36 mV dec^{-1}; j_0: 0.063 mA cm^{-2}	Electrolyte: H_2-bubbled 0.1 M $HClO_4$	15
Fe-WCN	η_o: 100 mV; η_{10}: 220 mV; Tafel slope: 47.1 mV dec^{-1}	Electrolyte: H_2SO_4 (pH 1); Scan rate=5 mV s^{-1}	16
CNS@WC/GF	η_{10}: 65 mV; Tafel slope: 61 mV dec^{-1}; j_0: 7.58 × 10^{-2} mA cm^{-2}	Electrolyte: 1 M H_2SO_4; Scan rate: 2 mV s^{-1}	This work

Table S2 Summary of catalytic performance of tungsten carbide-based HER catalysts in alkaline solutions

Sample	Catalytic performance	Experimental conditions	Ref.
WC-CNTs	η_o: 16 mV; η_{10}: 137 mV; $j_{300\ mV}$: 33.1 mA cm^{-2}; Tafel slope: 106 mV dec^{-1}	Electrolyte: 0.1 M KOH; Scan rate: 50 mV s^{-1}	3
WC/flake Ni	j_0: 4.02 *10^{-4} A cm^{-2}; Tafel slop: 133 mV dec^{-1}	Electrolyte: 6 M KOH; Scan rate: 5 mV s^{-1}	8
WC/foam Ni	j_0: 4.22*10^{-4} A cm^{-2}; Tafel slop: 125 mV dec^{-1}		8
Carbon coated cobalt–tungsten carbide Co_6W_6C	η_{10}: 73 mV; Tafel slope:25 mV dec^{-1}; j_0: 0.0412 mA cm^{-2}	Electrolyte: 1 M KOH; Scan rate: 50 mV s^{-1}	14
Fe-WCN	η_o: 120 mV; η_{10}: 250 mV; Tafel slope: 47.1 mV dec^{-1}	Electrolyte: alkaline medium (pH: 13); Scan rate: 5 mV s^{-1}	16
CNS@WC/GF	η_{10}: 68 mV; Tafel slope: 72 mV dec^{-1}; j_0: 5.37 × 10^{-2} mA cm^{-2}	Electrolyte: 1 M KOH; Scan rate: 2 mV s^{-1}	This work

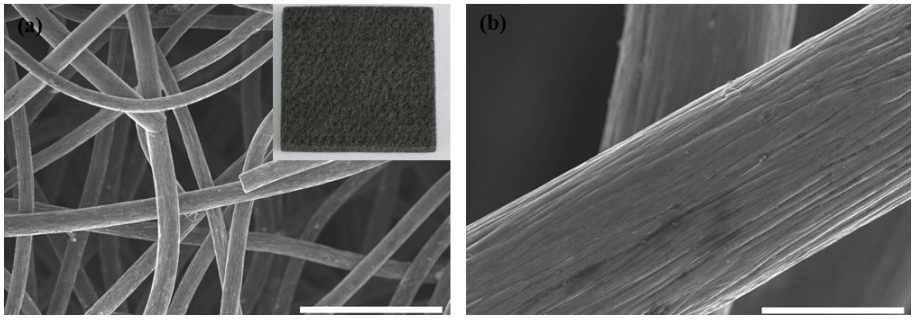

Fig. S1 FESEM micrographs of pristine carbon felt (Inset in (a) is an optical image of a piece of 5 × 5 × 0.5 cm carbon felt sheet.) Scale bars, 100 μm (a), 10 μm (b)

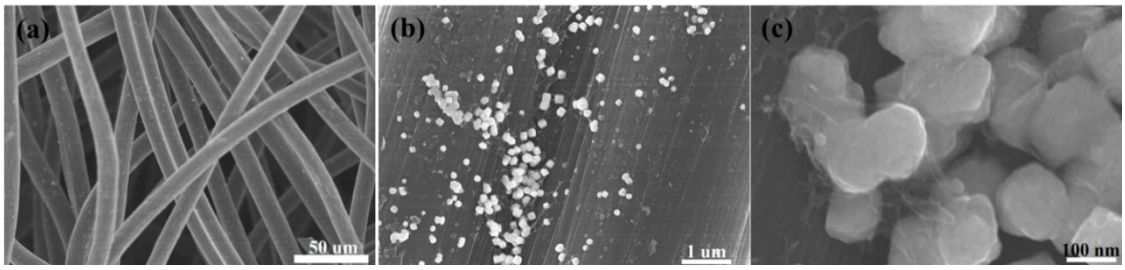

Fig. S2 FESEM micrographs of CNS@WC/GF with various magnifications.

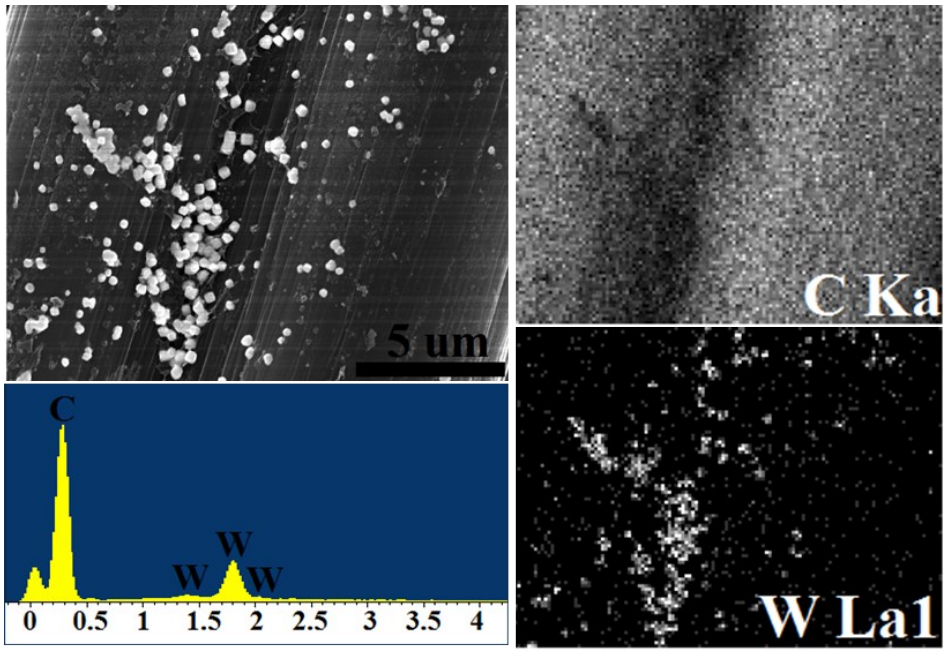

Fig. S3 EDX analyses of CNS@WC/GF.

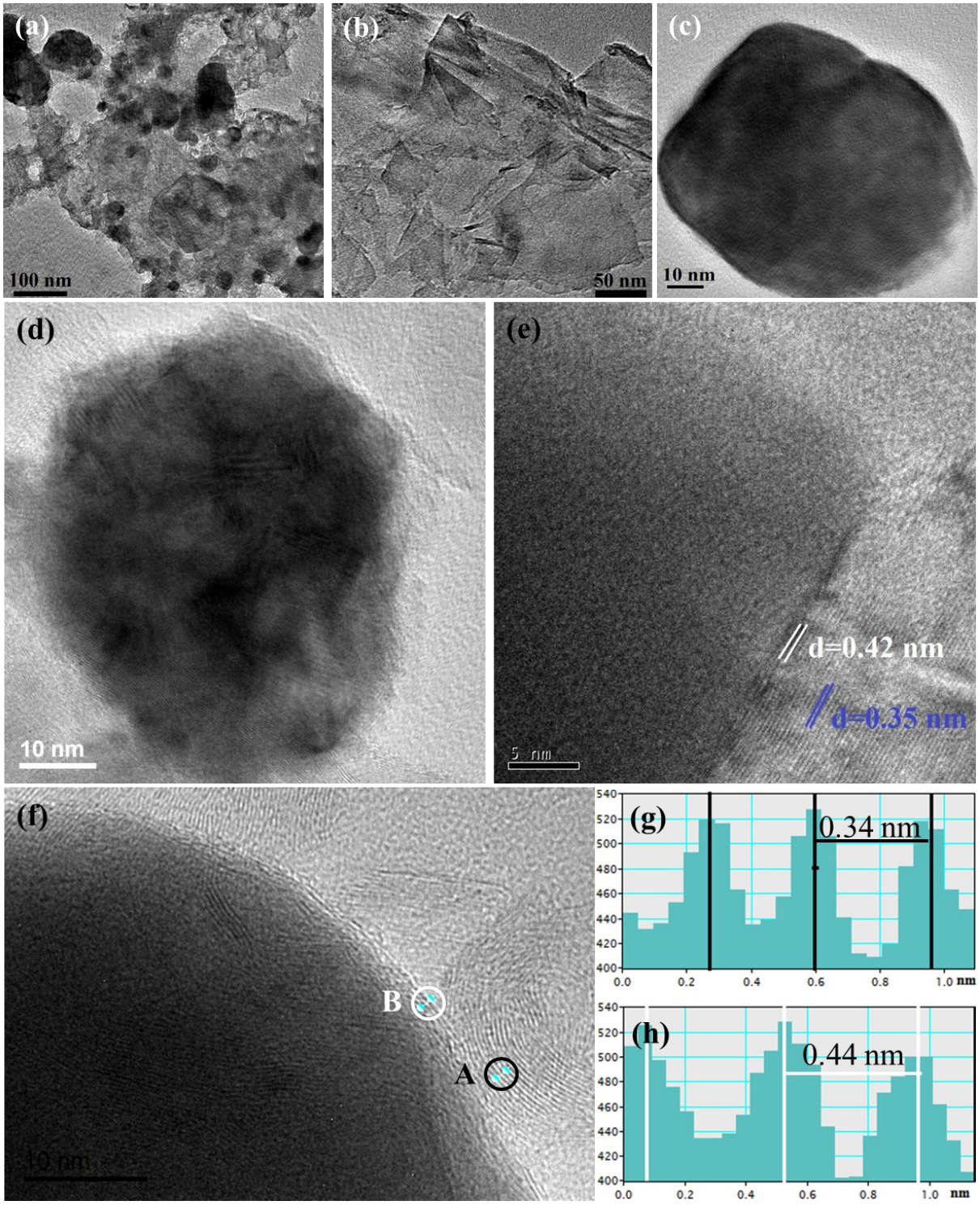

Fig. S4 TEM micrographs of CNS@WC/GF (a), CNS (b), CNS@WC nanoparticles (c, d), high-resolution TEM micrographs (e, f) and the corresponding line profiles (g, h) of spots A and B in (c).

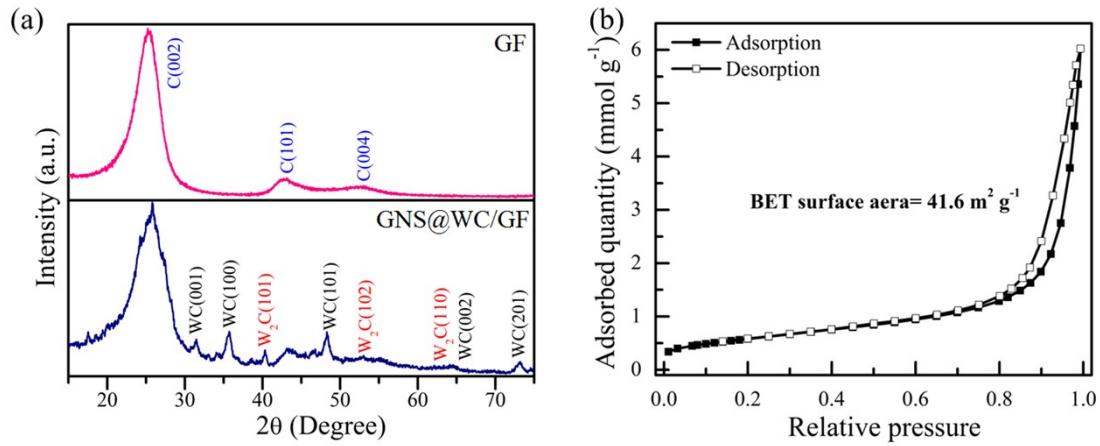

Fig. S5 XRD patterns of GF and CNS@WC/GF (a), and N2 absorption-desorption isotherm of CNS@WC/GF.

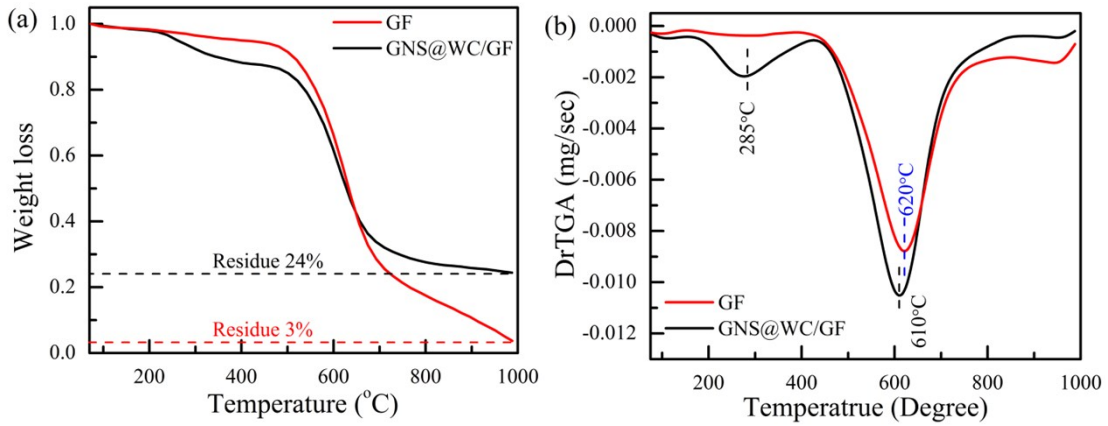

Fig. S6 TGA (a) and derivative TGA (b) curves of GF and CNS@WC/GF.

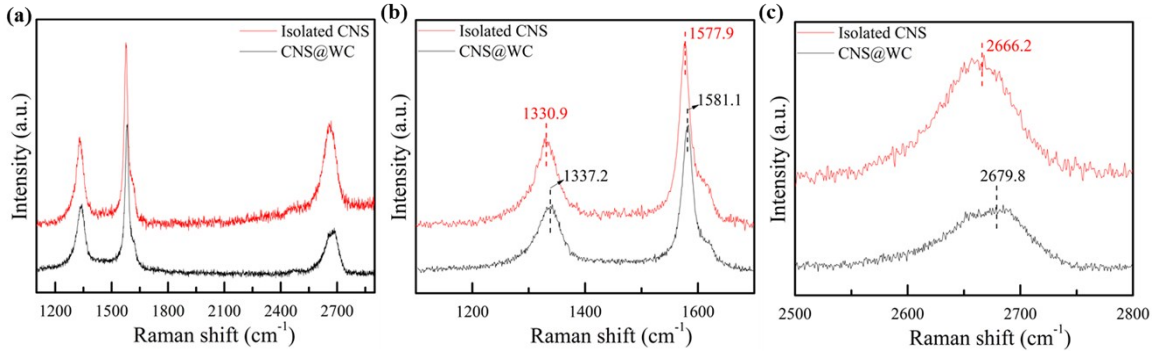

Fig. S7 Raman spectra of isolated carbon nanosheets and CNS@WC, (a) overall view, (b) D and G bands, and (c) 2D band.

Table R1 Results of Raman analysis (For each sample, at least five tests were conducted at different locations. The average values together with standard deviations are presented. The intensity values were obtained by integrating the corresponding peaks.

Sample	D band			G band			2D band			I_G/I_{2D}
	Positon	Intensity	fwhm	Positon	Intensity	fwhm	Positon	Intensity	fwhm	
CNS	1331±4.6	248699±5296	54±2.1	1577±7.6	262322±6211	19±2.2	2664±3.8	440661±9002	75±2.3	0.6
CNS@WC	1336±5.2	165441±7483	53±1.2	1580±3.1	176915±6589	18±1.4	2678±6.7	225115±8113	92±2.1	0.8

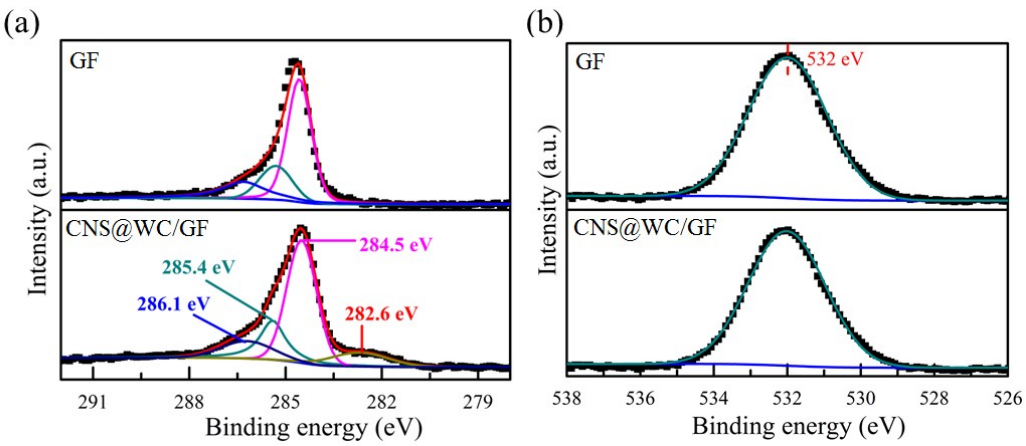

Fig. S8 XPS spectra of C 1s (a), and O 1s (b) of GF and CNS@WC/GF.

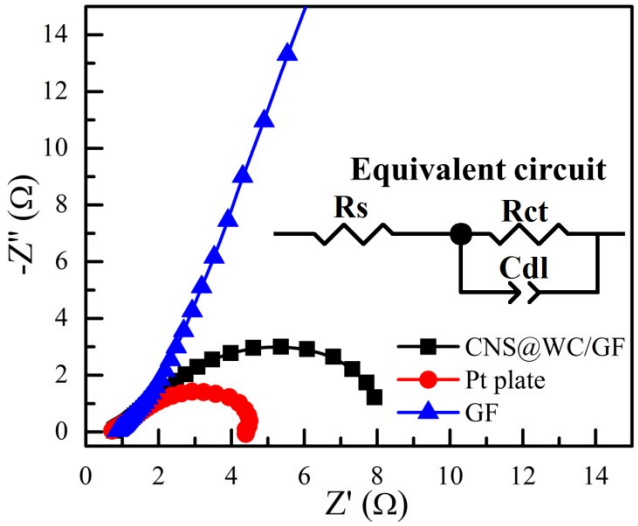

Fig. S9 Nyquist plots of catalysts and the equivalent circuit

Reference

1. Y. Shen, A. C. Lua, Appl. Catal., B 2015, 164, 61–69
2. Y. Shen, A. C. Lua, J. Xi, X. Qiu, ACS Appl. Mater. Interfaces DOI: 10.1021/acsami.5b11966
3. X .J. Fan, H. Q. Zhou, X. Guo, ACS Nano 2015, 9, 5125-5134
4. H. L. Fei, Y. Yang, X. J. Fan, G. Wang, G. D. Ruan, J. M. Tour, J. Mater. Chem. A 2015, 3, 5798–5804
5. W.-F. Chen, J. M. Schneider, K. Sasaki, C.-H. Wang, J. Schneider, S. Iyer, S. Iyer, Y. M. Zhu, J. T. Muckerman, E. Fujita, ChemSusChem 2014, 7, 2414–2418
6. C. Y. Tang, D. Z. Wang, Z. Z. Wu, B. H. Duan, Int. J. Hydrogen Energy 2015, 40, 3229-3237

7. J.-F. Lin, O. Pitkanen, J. Maklin, R. Puskas, A. Kukovecz, A. Dombovari, G. Toth, K. Kordas, J. Mater. Chem. A, 2015,3, 14609–14616
8. H. J. Zheng, J. G. Huang, W. Wang, C. N. Ma, Electrochem. Commun. 2005, 7 1045–1049
9. P. Xiao, X. M. Ge, H. B. Wang, Z. L Liu, A. Fisher, and X. Wang, Adv. Funct. Mater. 2015, 25, 1520–1526
10. Y. Yan, B. Y. Xia, X. Y. Qi, H. B. Wang, R. Xu, J.-Y. Wang, H. Zhang and X. Wang, Chem. Commun. 2013, 49, 4884–4886
11. S. T. Hunt, T. Nimmanwudipong, Y. Romn-Leshkov, Angew. Chem. Int. Ed. 2014, 53, 5131 –5136
12. S. Wirth, F. Harnisch, M. Weinmann, U. Schröder, Appl. Catal. B, 2012, 126, 225– 230
13. Y. N. Regmi, G. R. Waetzig, K. D. Duffee, S. M. Schmuecker, J. M. Thode and B. M. Leonard, J. Mater. Chem. A, 2015, 3, 10085–10091
14. Y. P. Liu, G.-D. Li, L. Yuan, L. Ge, H. Ding, D. J. Wang and X. X. Zou, Nanoscale 2015, 7, 3130–3136
15. F. K. Meng, E. Y. Hu, L. H. Zhang, K. Sasaki, J. T. Muckerman and E. Fujita. J. Mater. Chem. A, 2015, 3, 18572–18577
16. Y. Zhao, K. Kamiya, K. Hashimoto, S. Nakanishi, Angew. Chem. Int. Ed.2013, 52, 13638 –13641